

A short survey on QPSK Costas loop mathematical models

Kuznetsov N.V.*** Kuznetsova O.A.* Leonov G.A.**
Yuldashev M.V.* Yuldashev R.V.*

* Faculty of Mathematics and Mechanics, Saint-Petersburg State University, Russia

** Dept. of Mathematical Information Technology, University of Jyväskylä, Finland (e-mail: nkuznetsov239@gmail.com)

*** Institute for Problems in Mechanical Engineering of the Russian Academy of Sciences, Russia

Abstract: The Costas loop is a modification of the phase-locked loop circuit, which demodulates data and recovers carrier from the input signal. The Costas loop is essentially a nonlinear control system and its nonlinear analysis is a challenging task. Thus, simplified mathematical models and their numerical simulation are widely used for its analysis. At the same time for phase-locked loop circuits there are known various examples where the results of such simplified analysis are differ substantially from the real behavior of the circuit. In this survey the corresponding problems are demonstrated and discussed for the QPSK Costas loop.

Keywords: QPSK Costas loop, PLL, phase-locked loop, simulation, nonlinear analysis

1. INTRODUCTION

The Costas loop is a classical modification of the phase-locked loop circuit (PLL), which is a nonlinear control system designed to generate an electrical signal, the phase of which is automatically tuned to the phase of the input signal. The Costas loop is essentially a nonlinear control system and its nonlinear analysis is a challenging task. Thus, simplified mathematical models and their numerical simulation are widely used for its analysis. At the same time for PLL based circuits there are known various examples where the results of such simplified analysis are differ substantially from the real behavior of the circuit (see corresponding discussion of gaps between mathematical control theory, the theory of dynamical systems and the engineering practice of PLL in (Leonov et al., 2015)). Recently such examples were discussed for the BPSK Costas loop in (Best et al., 2015, 2016). In this survey the corresponding problems are revealed and discussed for the QPSK Costas loop.

2. QPSK COSTAS LOOP OPERATION

Consider the Quadrature Phase Shift Keying Costas loop (QPSK Costas loop) after transient processes (see Fig. 1). The input QPSK signal has the form

$$m_1(t) \cos(\omega t) + m_2(t) \sin(\omega t),$$

where $m_{1,2}(t) = \pm 1$ is data signal, $\sin(\omega t)$ and $\cos(\omega t)$ are sinusoidal carriers, $\theta_{\text{ref}}(t) = \omega t$ — phase of input signal. The VCO has two outputs with 90° phase difference: $\cos(\omega t - \theta_\Delta)$ and $\sin(\omega t - \theta_\Delta)$, with $\theta_{\text{vco}}(t) = \omega t - \theta_\Delta$ — their phase.

After multiplication of VCO signal and the input signal by multiplier block (\otimes) on the upper branch one has

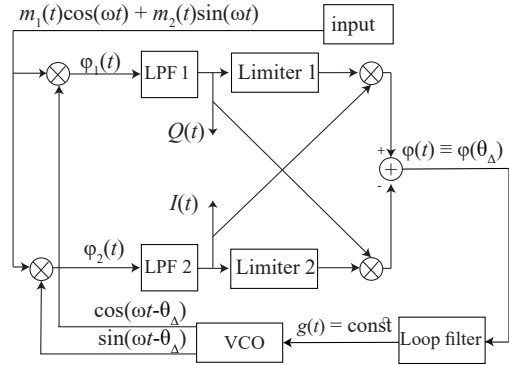


Fig. 1. QPSK Costas loop after transient process.

$$\varphi_1(t) = \left(m_1(t) \cos(\omega t) + m_2(t) \sin(\omega t) \right) \cos(\omega t - \theta_\Delta).$$

On the lower branch the output signal of VCO is multiplied by the input signal:

$$\varphi_2(t) = \left(m_1(t) \cos(\omega t) + m_2(t) \sin(\omega t) \right) \sin(\omega t - \theta_\Delta).$$

Assumption 1. The initial states of filters $x_1(0)$, $x_2(0)$, and $x(0)$ do not affect the synchronization of the loop (since for the properly designed filters, the impact of filter's initial state on its output decays exponentially with time).

Assumption 1 allows one to consider the dependence of the filter output only on its input ignoring its internal state (see Fig. 2).

Assumption 2 The terms, whose frequency is about twice the carrier frequency, do not affect the synchronization of the loop (since they are supposed to be completely suppressed by the low-pass filters).

Here, from an engineering point of view, the high-frequency terms ($\cos(2\omega t - \theta_\Delta)$ and $\sin(2\omega t - \theta_\Delta)$) are removed by ideal low-pass filters LPF 1 and LPF 2. Therefore the consideration of such approximations doesn't change the outputs of low-pass filter and is not essential for the analysis of synchronization.

In this case, by Assumption 1 the signals $Q(t)$ and $I(t)$ on the upper and lower branches can be approximated as

$$\begin{aligned} Q(t) &\approx \frac{1}{2} \left(m_1(t) \cos(\theta_\Delta) + m_2(t) \sin(\theta_\Delta) \right), \\ I(t) &\approx \frac{1}{2} \left(-m_1(t) \sin(\theta_\Delta) + m_2(t) \cos(\theta_\Delta) \right). \end{aligned} \quad (1)$$

For small values of θ_Δ we get demodulated data

$$Q(t) \approx \frac{1}{2} m_1(t), \quad I(t) \approx \frac{1}{2} m_2(t). \quad (2)$$

Consider Costas loop before synchronization (see Fig. 2)

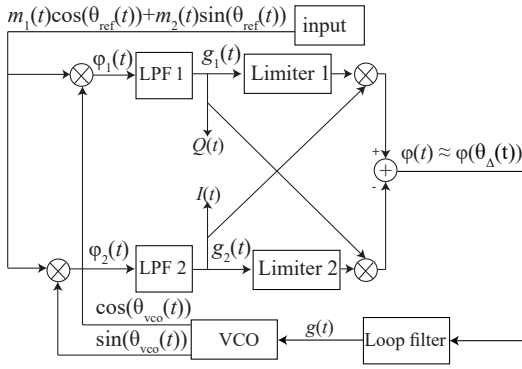


Fig. 2. QPSK Costas loop before synchronization.

in the case when the phase difference is not constant:

$$\theta_\Delta(t) = \theta_{\text{ref}}(t) - \theta_{\text{vco}}(t) \neq \text{const}. \quad (3)$$

Caveat to Assumption 2. While Assumption 2 is reasonable from a practical point of view, its use in the analysis of Costas loop requires further consideration (see, e.g., (Piqueira and Monteiro, 2003)). Here the application of averaging methods allows one to justify Assumption 2 and obtain the conditions under which Assumption 2 can be used (see, e.g., (Leonov et al., 2012, 2016)).

After the filtration, both signals $\varphi_1(t)$ and $\varphi_2(t)$ pass through the limiters. Then the outputs of the limiters $\text{sign}(Q(t))$ and $\text{sign}(I(t))$ are multiplied by $I(t)$ and $Q(t)$. By Assumption 2 and corresponding formula (1) the difference of these signals

$$\varphi(t) = I(t)\text{sign}(Q(t)) - Q(t)\text{sign}(I(t)) \quad (4)$$

can be approximated as

$$\begin{aligned} \varphi(t) &\approx \frac{1}{2} \left(-m_1(t) \sin(\theta_\Delta(t)) + m_2(t) \cos(\theta_\Delta(t)) \right) \\ &\text{sign} \left(m_1(t) \cos(\theta_\Delta(t)) + m_2(t) \sin(\theta_\Delta(t)) \right) - \\ &- \frac{1}{2} \left(m_1(t) \cos(\theta_\Delta(t)) + m_2(t) \sin(\theta_\Delta(t)) \right) \\ &\text{sign} \left(-m_1(t) \sin(\theta_\Delta(t)) + m_2(t) \cos(\theta_\Delta(t)) \right) = \\ &= \varphi(\theta_\Delta(t)) = \begin{cases} -\sin(\theta_\Delta(t)), & -\frac{\pi}{4} < \theta_\Delta(t) < \frac{\pi}{4}, \\ \cos(\theta_\Delta(t)), & \frac{\pi}{4} < \theta_\Delta(t) < \frac{3\pi}{4}, \\ \sin(\theta_\Delta(t)), & \frac{3\pi}{4} < \theta_\Delta(t) < \frac{5\pi}{4}, \\ -\cos(\theta_\Delta(t)), & \frac{5\pi}{4} < \theta_\Delta(t) < -\frac{\pi}{4}. \end{cases} \end{aligned} \quad (5)$$

Here $\varphi(\theta_\Delta(t))$ is a piecewise-smooth function. It should be noted, that function $\varphi(\theta_\Delta(t))$ depends on $m_{1,2}$ in points $\theta_\Delta = \pm \frac{\pi}{4}, \pm \frac{3\pi}{4}$.

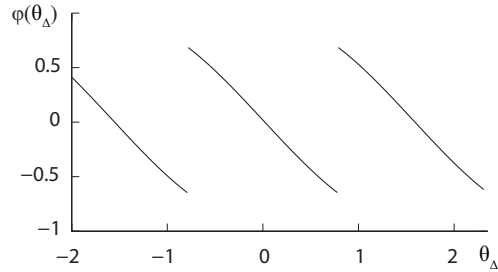


Fig. 3. Phase detector characteristic of QPSK Costas loop $\varphi(\theta_\Delta)$.

The resulting signal $\varphi(t)$ after the filtration by the loop filter forms the control signal $g(t)$ for the VCO.

Assumption 3. The data signals $m_{1,2}(t)$ do not affect the synchronization of the loop.

Assumptions 1–3 together lead to the concept of so-called *ideal low-pass filter*. It removes the upper sideband, whose frequency is about twice carrier frequency (Assumption 2), and passes the lower sideband without change (Assumptions 1,3). Thus it is assumed that the lower sideband of $\varphi_1(t)$ and $\varphi_2(t)$ are passed without changes and the transmitted data $m_{1,2}(t)$ is neglected in the signal $\varphi(t)$ (see equation (5)). For $m_{1,2}(t) \equiv \text{const}$ approximations (1) depend on the phase difference of signals only, i.e. two multiplier blocks (\otimes) on the upper and lower branches operate as phase detectors.

Caveat to Assumption 3. Low-pass filters can not operate perfectly at moments of changing $m_{1,2}(t)$, therefore the data pulse shapes are no longer ideal rectangular pulses after filtration due to distortion, created by the low-pass filters. This can lead to incorrect conclusions on the performance of the loop. One of known examples is so-called false-lock: while for $m_{1,2}(t) \equiv \text{const}$ the loop acquires lock and proper synchronization of the carrier and VCO frequencies, for time-varying $m(t) \neq \text{const}$ the loop can acquire lock without proper synchronization of the frequencies (false lock) (Olson, 1975; Simon, 1978; Hedin et al., 1978). To avoid such undesirable situation one may try to choose loop parameters in such a way that the synchronization time is less than the time between changes

in the data signal $m_{1,2}(t)$ or to modify the loop design (see, e.g., (Olson, 1975)). Another way is to perform the nonlinear nonlocal analysis of the loop (see, e.g., (Stensby, 1989, 2002)) to identify unsuitable parameters.

Caveat to Assumption 1. If in Fig. 2 the loop is out of lock, i.e. synchronization is not achieved, filters' initial states cannot be ignored and must be taken into account. Really, low-pass filters with nonzero initial states may change the lower sideband (see expressions (1)) and affect the synchronization of the loop. For rigorous consideration of low-pass filters one has to use mathematical models of filters instead of approximations (1). Since the low-pass filters LPF 1 and LPF 2 are mostly used for data demodulation, the effect of nonzero initial state of filter on transient processes will be discussed for the loop filter, which is used to provide synchronization.

The relation between the input $\varphi(t)$ and the output $g(t)$ of the Loop filter has the form

$$\frac{dx}{dt} = Ax + b\varphi(t), \quad g(t) = c^*x + h\varphi(t). \quad (6)$$

Here A is a constant matrix, vector $x(t)$ is a filter state, b, c are constant vectors, and $x(0)$ is initial state of filter. The solution of equation (6) with initial data $x(0)$ (filter initial state) is as follows

$$g(t) = \alpha_0(t) + h\varphi(t) + \int_0^t \gamma(t-\tau)\varphi(\tau)d\tau. \quad (7)$$

Here $\gamma(t-\tau) = c^*e^{A(t-\tau)}b$ is an impulse response function of filter and $\alpha_0(t) = \alpha_0(t, x(0)) = c^*e^{At}x(0)$ is an exponentially damped function (i.e. the matrix A is stable). Corresponding transfer function takes the form¹

$$H(s) = -c^*(A - sI)^{-1}b + h. \quad (8)$$

The control signal $g(t)$ is used to adjust VCO frequency to the frequency of input carrier signal

$$\dot{\theta}_{\text{vco}}(t) = \omega_{\text{vco}}(t) = \omega_{\text{vco}}^{\text{free}} + K_{\text{vco}}g(t). \quad (9)$$

Here $\omega_{\text{vco}}^{\text{free}}$ is free-running frequency of VCO and K_{vco} is VCO gain. Note that the initial VCO frequency (at $t = 0$) is as follows

$$\omega_{\text{vco}}(0) = \omega_{\text{vco}}^{\text{free}} + K_{\text{vco}}\alpha_0(0) + K_{\text{vco}}h\varphi(\theta_{\Delta}(0)) \neq \omega_{\text{vco}}^{\text{free}}. \quad (10)$$

If the frequency of input carrier is a constant

$$\dot{\theta}_{\text{ref}}(t) = \omega_{\text{ref}}(t) \equiv \omega_{\text{ref}}, \quad (11)$$

then equations (4)-(9) give the following mathematical model of Costas loop

$$\begin{aligned} \dot{\theta}_{\Delta} &= \omega_{\text{ref}} - \omega_{\text{vco}}^{\text{free}} - K_{\text{vco}}\alpha_0(t) - \\ &- K_{\text{vco}}\left(h\varphi(\theta_{\Delta}) + \int_0^t \gamma(t-\tau)\varphi(\theta_{\Delta}(\tau))d\tau\right). \end{aligned} \quad (12)$$

Assumption 4 (Corollary 1 of Assumption 1). *Free output of loop filter $\alpha_0(t)$ does not affect the synchronization of the loop since $\alpha_0(t)$ is an exponentially damped function.*

¹ In the control theory (Leonov and Kuznetsov, 2014) it is defined with opposite sign: $c^*(A - sI)^{-1}b - h$

For $h = 0$ Assumption 4 allows one to obtain the classical mathematical model of Costas loop (see Fig. 4)

$$\dot{\theta}_{\Delta} = \omega_{\Delta}^{\text{free}} - K_{\text{vco}} \int_0^t \gamma(t-\tau)\varphi(\theta_{\Delta}(\tau))d\tau \quad (13)$$

$$\theta_{\Delta}(t) = \theta_{\text{ref}}(t) - \theta_{\text{vco}}(t), \quad \omega_{\Delta}^{\text{free}} = \omega_{\text{ref}} - \omega_{\text{vco}}^{\text{free}}$$

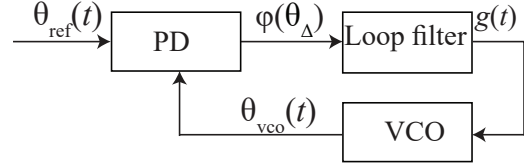


Fig. 4. Classical mathematical model of QPSK Costas loop.

Caveat to Assumption 4. For high-order filter, two different initial states $\tilde{x}(0)$ and $\tilde{\tilde{x}}(0)$ may lead to identical values of $\alpha_0(0, \tilde{x}(0)) = \alpha_0(0, \tilde{\tilde{x}}(0))$ but different functions $\alpha_0(t, \tilde{x}(0))$ and $\alpha_0(t, \tilde{\tilde{x}}(0))$ (to avoid this effect it is necessary to assume the observability of system (6)).

Since nonlinear mathematical model of Costas loop (13) is hard to analyze, in practice, for its analysis it is widely used numerical simulation and linearization. In the case when the phase difference of signals is small one can consider a linearized mathematical model of Costas loop, using the linearization $\varphi(\theta_{\Delta}) \approx K\theta_{\Delta}$. This allows one to estimate hold-in range by the same methods that were developed for analysis and design of classical PLLs (see, e.g., (Gardner, 1966; Viterbi, 1966; Lindsey, 1972; Shakhgil'dyan and Lyakhovkin, 1972), and others). Linearized model (12), where $\varphi(\Delta\theta)$ is changed by $K\theta_{\Delta}$, may be used for analysis in the case when the loop is in lock, but analysis of the acquisition behavior cannot be accomplished using linearized models.

Next we discuss rigorous derivation of nonlinear mathematical model. The relation between the inputs $\varphi_{1,2}(t)$ and the outputs $g_1(t) = Q(t)$ and $g_2(t) = I(t)$ of the low-pass filters is similar to (6):

$$\frac{dx_{1,2}}{dt} = A_{1,2}x_{1,2} + b_{1,2}\varphi_{1,2}(t), \quad g_{1,2}(t) = c_{1,2}^*x_{1,2}. \quad (14)$$

Here $A_{1,2}$ are constant matrices, the vectors $x_{1,2}(t)$ are filter states, $b_{1,2}, c_{1,2}$ are constant vectors, and $x_{1,2}(0)$ are initial states of filters.

Then, taking into account (14), (6), and (9), one obtains *mathematical model in the signal space* describing *physical model* of QPSK Costas loop:

$$\begin{aligned} \dot{x}_1 &= A_1x_1 + \\ &+ b_1 \cos(\theta_{\text{vco}})(m_1(t) \cos(\theta_{\text{ref}}(t)) + m_2(t) \sin(\theta_{\text{ref}}(t))), \\ \dot{x}_2 &= A_2x_2 + \\ &+ b_2 \sin(\theta_{\text{vco}})(m_1(t) \cos(\theta_{\text{ref}}(t)) + m_2(t) \sin(\theta_{\text{ref}}(t))), \\ \dot{x} &= Ax + b(\text{sign}(c_1^*x_1)(c_2^*x_2) - \text{sign}(c_2^*x_2)(c_1^*x_1)), \\ \dot{\theta}_{\text{vco}} &= \omega_{\text{vco}}^{\text{free}} + K_{\text{vco}}(c^*x) + \\ &+ K_{\text{vco}}((c_2^*x_2)\text{sign}(c_1^*x_1) - (c_1^*x_1)\text{sign}(c_2^*x_2)). \end{aligned} \quad (15)$$

Here $\theta_{\text{vco}}(0)$ is the initial phase shift of VCO and the vectors $x_{1,2}(0), x(0)$ are initial states of filters (so Assumptions 2 and 4 are not used). Thus the initial VCO frequency (at $t = 0$) has the form

$$\begin{aligned} \omega_{\text{vco}}(0) &= \omega_{\text{vco}}^{\text{free}} + K_{\text{vco}}c^*x(0) + \\ &+ K_{\text{vco}}((c_2^*x_2(0))\text{sign}(c_1^*x_1(0)) - (c_1^*x_1(0))\text{sign}(c_2^*x_2(0))). \end{aligned} \quad (16)$$

Right-hand side of (16) is discontinuous. Fig. 5 shows function $y_1\text{sign}(y_2) - y_2\text{sign}(y_1)$ around zero.

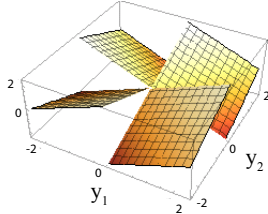


Fig. 5. Plot of the function $y_1\text{sign}(y_2) - y_2\text{sign}(y_1)$.

The mathematical model in signal space (15) is nonlinear nonautonomous discontinuous differential system, so in general case its analytical study is a difficult task even for the continuous case when $m_{1,2}(t) \equiv \text{const}$. Moreover it is a slow-fast system, so its numerical study is rather complicated for the high-frequency signals. The problem is that it is necessary to consider simultaneously both very fast time scale of the signals $\sin(\theta_{1,2}(t))$ and slow time scale of phase difference between the signals $\theta_{\Delta}(t)$, therefore one very small simulation time-step must be taken over a very long total simulation period (Goyal et al., 2006; Kuznetsov et al., 2014).

To overcome these problems in PLL and classic Costas loop, in place of using Assumption 2 one can apply averaging methods (Krylov and Bogolyubov, 1947; Mitropolsky and Bogolubov, 1961; Samoilenko and Petryshyn, 2004; Sanders et al., 2007) and consider a *simplified mathematical model in the signal's phase space*. Remark that classical averaging approach requires Lipschitz condition, which is not satisfied in the case of QPSK Costas loop system.

It is useful to formalize engineering Assumption 2 and the explanation of low-pass filters operation in the following way

$$\begin{aligned} \int_{t_0}^t \gamma_{1,2}(t-\tau) \sin \theta(\tau) d\tau &= \\ &= \sin(\theta(t)) + O\left(\frac{1}{\omega_{\min}}\right), \quad \forall \dot{\theta}(t) < \omega_{\Delta}^{\max}, \\ \int_{t_0}^t \gamma_{1,2}(t-\tau) \sin \theta(\tau) d\tau &= O\left(\frac{1}{\omega_{\min}}\right), \\ \forall \dot{\theta}(t) > \frac{C}{\sqrt{\omega_{\min}}}, \\ \gamma_{1,2}(t-\tau) &= c_{1,2}^* e^{A_{1,2}(t-\tau)} b_{1,2}, \\ \alpha_{1,2}(t) &= c_{1,2}^* e^{A_{1,2}t} x_{1,2}(0). \end{aligned} \quad (17)$$

Here $\omega_{\text{vco, ref}}(t) > \omega^{\min} > 0$, $1/\sqrt{\omega^{\min}} < |\omega_{\text{ref}}(t) - \omega_{\text{vco}}(t)| < \omega_{\Delta}^{\max}$ on sufficiently large time interval, t_0 is a moment of time such that $\alpha_{1,2}(t) \leq \frac{1}{\omega^{\min}}$ for $t > t_0$. If the

initial states of low-pass filters LPF 1 and LPF 2 are zero, then $\alpha_1(t) = \alpha_2(t) = 0$ (see Assumption 1, Assumption 4).

Applying (17) to (15), one obtains

$$\begin{aligned} \dot{x} &= Ax + b\varphi(\theta_{\Delta}), \\ \dot{\theta}_{\Delta} &= \omega_{\Delta}^{\text{free}} - K_{\text{vco}}(c^*x) - K_{\text{vco}}h\varphi(\theta_{\Delta}), \\ \varphi(\theta_{\Delta}) &= \frac{1}{\sqrt{2}} \left(\sin(\theta_{\Delta}(\tau) + \frac{\pi}{4}) \right. \\ &\quad \left. \text{sign}\left(\sin(\theta_{\Delta}(t) - \frac{\pi}{4})\right) - \right. \\ &\quad \left. - \sin(\theta_{\Delta}(\tau) - \frac{\pi}{4}) \right. \\ &\quad \left. \text{sign}\left(\sin(\theta_{\Delta}(t) + \frac{\pi}{4})\right) \right) + O\left(\frac{1}{\sqrt{\omega_{\min}}}\right). \end{aligned} \quad (18)$$

Corresponding detailed discussion can be found in (Leonov et al., 2016).

Assumption 5 (Corollary of Assumptions 1-3). *Solutions of system (15) under condition (17) are close to the solutions of the following system (i.e. $O(\frac{1}{\sqrt{\omega_{\min}}})$ can be neglected)*

$$\begin{aligned} \dot{x} &= Ax + b\varphi(\theta_{\Delta}), \\ \dot{\theta}_{\Delta} &= \omega_{\Delta}^{\text{free}} - K_{\text{vco}}c^*x - K_{\text{vco}}h\varphi(\theta_{\Delta}), \\ \varphi(\theta_{\Delta}) &= \frac{1}{\sqrt{2}} \left(\right. \\ &\quad \left. \sin(\theta_{\Delta}(\tau) + \frac{\pi}{4})\text{sign}\left(\sin(\theta_{\Delta}(t) - \frac{\pi}{4})\right) - \right. \\ &\quad \left. - \sin(\theta_{\Delta}(\tau) - \frac{\pi}{4})\text{sign}\left(\sin(\theta_{\Delta}(t) + \frac{\pi}{4})\right) \right). \end{aligned} \quad (19)$$

Here function $\varphi(\theta_{\Delta})$ is a phase detector characteristic of QPSK Costas loop for sinusoidal signals, which is used in classical books. Note that here the phase detector operation include operations of multipliers, limiters, LPF 1, and LPF 2.

Let us determine equilibrium points. Consider a transfer function of the capacitor-based filter without parasitic resistance

$$F(s) = \frac{1}{Cs}. \quad (20)$$

System (19) with this filter takes the following form

$$\begin{aligned} \dot{x} &= \frac{1}{C}\varphi(\theta_{\Delta}), \\ \dot{\theta}_{\Delta} &= \omega_{\Delta}^{\text{free}} - Lx. \end{aligned} \quad (21)$$

This system has the following equilibrium points

$$x = \frac{\omega_{\Delta}^{\text{free}}}{L}, \quad \varphi(\theta_{\Delta}) = 0. \quad (22)$$

If A is a non-singular matrix, then equilibrium points are determined by the following system

$$\begin{aligned} x &= A^{-1}b\varphi(\theta_{\Delta}), \\ \varphi(\theta_{\Delta}) &= \frac{\omega_{\Delta}^{\text{free}}}{(K_{\text{vco}}c^*A^{-1}b + K_{\text{vco}}h)}. \end{aligned} \quad (23)$$

Denote

$$\gamma = \frac{\omega_{\Delta}^{\text{free}}}{(K_{\text{vco}}c^*A^{-1}b + K_{\text{vco}}h)}. \quad (24)$$

Then

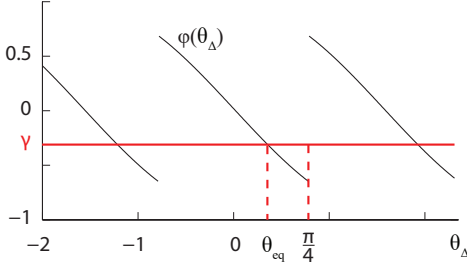


Fig. 6. Equilibrium points of QPSK Costas loop with filter without 0 poles.

$$\theta_{eq} = -\arcsin\left(\frac{\omega_{\Delta}^{\text{free}}}{L(c^*A^{-1}b+h)}\right) + \pi k. \quad (25)$$

The linearized system in the neighborhood of θ_{eq} is as follows

$$\begin{aligned} \dot{x} &= Ax - b \cos(\theta_{eq})\theta_{\Delta-eq}, \\ \dot{\theta}_{\Delta-eq} &= \omega_{\Delta}^{\text{free}} - K_{\text{vco}}c^*x + K_{\text{vco}}\cos(\theta_{eq})\theta_{\Delta-eq}, \\ \theta_{\Delta-eq} &= \theta_{\Delta} - \theta_{eq} \end{aligned} \quad (26)$$

Using equality

$$\det \begin{pmatrix} A & B \\ C & D \end{pmatrix} = \det A \cdot \det(D - CA^{-1}B), \quad (27)$$

one can obtain the characteristic polynomial

$$\begin{aligned} \chi(s) &= \det \begin{pmatrix} A - sI & -b \cos(\theta_{eq}) \\ -K_{\text{vco}}c^* & K_{\text{vco}}\cos(\theta_{eq}) - s \end{pmatrix} \\ &= \det(A - sI) \\ &= \det(A - sI)(K_{\text{vco}}\cos(\theta_{eq}) - s - K_{\text{vco}}c^*(A - sI)^{-1}b \cos(\theta_{eq})) \\ &= \det(A - sI)(K_{\text{vco}}\cos(\theta_{eq}) - s + LH(s)\cos(\theta_{eq})). \end{aligned} \quad (28)$$

Denote a filter transfer function $H(s) = \frac{M(s)}{N(s)}$. Then

$$\chi(s) = -N(s)(K_{\text{vco}}\cos(\theta_{eq}) - s) + M(s)L\cos(\theta_{eq}) \quad (29)$$

For the properly designed QPSK Costas Loop θ_{eq} is a stable point. If all of the zeros of the characteristic polynomial $\chi(s)$ have negative real parts, then θ_{eq} is asymptotically stable equilibrium point. Thus, the parameters of the filters (N , M , L , and h) should satisfy this rule.

Suppose that

$$-\frac{\pi}{4} + \pi n < \theta_{\Delta}(t) < \frac{\pi}{4} + \pi n. \quad (30)$$

Then the function $\varphi(t)$ becomes continuous, so it is possible to apply classical averaging theorem. Until the initial frequency difference is sufficiently large and (30) is not satisfied, one has to apply different approach to investigation of transient processes (Leonov et al., 2016).

Caveat to Assumption 5. For rigorous justification of Assumption 5 one has to prove that $O(\frac{1}{\sqrt{\omega_{min}}})$ does not affect the behaviour of Limiters.

3. COUNTEREXAMPLES TO THE ASSUMPTIONS

Note once more that various simplifications and the analysis of linearized models of control systems may result

in incorrect conclusions². At the same time the application of nonlinear methods for the analysis of PLL-based models are quite rare (see, e.g., (Abramovitch, 1990; Chang et al., 1993; Stensby, 1997; Shirahama et al., 1998; Watada et al., 1998; Hinz et al., 2000; Wu, 2002; Piqueira and Monteiro, 2003; Suarez and Quere, 2003; Margaris, 2004; Vendelin et al., 2005; Banerjee and Sarkar, 2006; Kudrewicz and Wasowicz, 2007; Wang et al., 2008; Bueno et al., 2010; Wiegand et al., 2010; Stensby, 2011; Suarez et al., 2012; Sarkar et al., 2014; Chicone and Heitzman, 2013; Yoshimura et al., 2013; Best et al., 2014)). Further examples demonstrate that the use of Assumptions 1-4 requires further study and rigorous justification. The following examples are shown that for the same parameters the operations of real *physical model* of Costas loop and *mathematical or physical simplified model*, taking into account one of the above Assumptions, may differ considerably.

Simulation model and parameters. In engineering practice one of the most popular way to describe linear filter is considering its transfer function $H(s)$ (see Fig. 7).

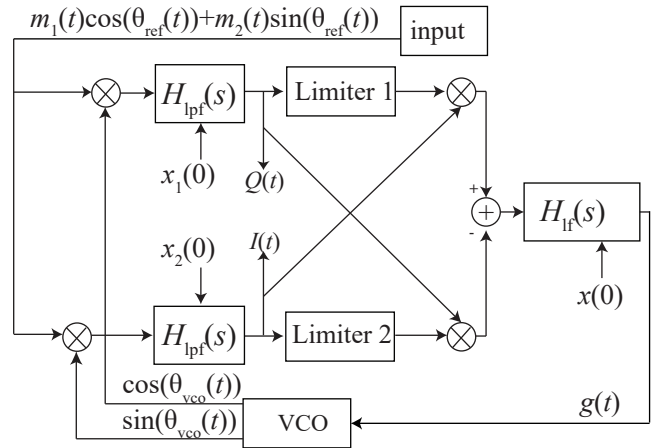


Fig. 7. QPSK Costas loop with filters defined by their transfer functions.

In the following examples we use loop filter transfer functions $H_{lf}(s) = \frac{\tau_2 s + 1}{\tau_1 s}$,

$$\tau_1 = 20 \cdot 10^{-6}, \tau_2 = 4 \cdot 10^{-6},$$

described by the equations

$$\begin{aligned} \dot{x} &= \xi, \\ \sigma &= \frac{1}{\tau_1}x + \frac{\tau_2}{\tau_1}\xi, \end{aligned} \quad (31)$$

where $\xi(t)$ is an input of the filter and $\sigma(t)$ is an output of the filter. Low pass filters transfer function is $H_{lpf}(s) = \frac{1}{s/\omega_{lpf} + 1}$, $\omega_{lpf} = 1.2566 \cdot 10^6$, and the corresponding equations are

$$\begin{aligned} \dot{x}_{1,2} &= -\omega_{lpf}x_{1,2} + \xi, \\ \sigma &= x_{1,2}, \end{aligned} \quad (32)$$

² see also counterexamples to the filter hypothesis, Aizerman's and Kalman's conjectures on the absolute stability of nonlinear control systems (Kuznetsov et al., 2011; Bragin et al., 2011; Leonov and Kuznetsov, 2013), and the Perron effects of the largest Lyapunov exponent sign inversions (Kuznetsov and Leonov, 2005; Leonov and Kuznetsov, 2007), etc.

where carrier frequency is $\omega_{\text{ref}} = 2 \cdot \pi \cdot 400000$, VCO input gain is $6.3165 \cdot 10^5$; VCO phase shift is zero; $m_2(t) = 1$;

Example 1. In Fig. 9 is shown that Assumptions 1 and 4 may not be valid: while physical model with zero initial states of low-pass filters acquire lock (black color), physical model with nonzero initial states of low-pass filters is out of lock (red color). It should be noted that in Fig. 9 initial frequencies of VCO corresponding to the red curve and black curve are the same. In Fig. 8 similar example is presented for nonzero initial state of loop filter.

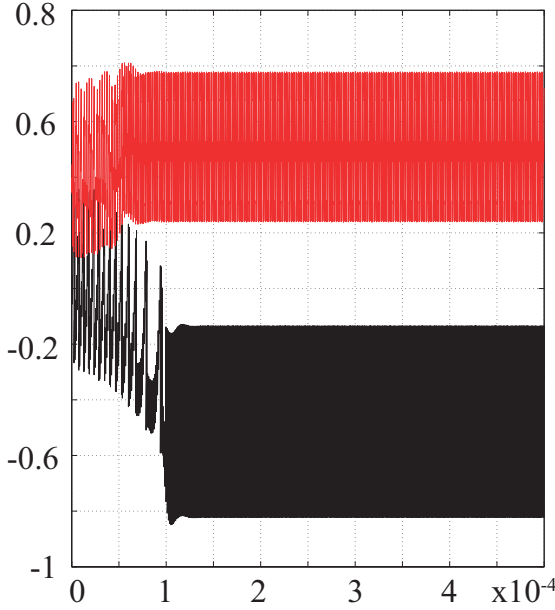


Fig. 8. Loop filter output: $m_1(t) = 1$; VCO free-running frequency is $2.6314 \cdot 10^6$ rad/s; VCO phase shift is zero; $\omega_{lpf} = 1.2566 \cdot 10^6$; initial loop filter state is 0.4 (red curve) and zero (black curve)

Example 2. In Fig. 10 is shown that Assumption 2 may not be valid: while averaged model acquire lock (black), physical model is out of lock (red).

Example 3. In Fig. 11 is shown that Assumption 3 may not be valid: while physical model (black) with constant data signal acquire lock, physical model (red) with non-constant data signal is out of lock.

Example 4. In Fig. 12 is shown that initial phase of VCO may affect stability of the loop: while physical model (black) with zero initial VCO phase acquires lock, physical model (red) with initial VCO phase equal to 0.8854 rad does not acquire lock.

Example 5. In Fig. 13 is shown that initial states of low-pass filters and initial phase difference may affect stability domain: while physical model with low-pass filters initial states $x_1(0) = 3$, $x_2(0) = 4.2566$ and zero is out of lock (red), classical mathematical model in the signal's phase space with initial phase shift $\theta_{\Delta}(0) = -\frac{\pi}{4}$ rad acquires lock (black). Therefore the consideration of classical mathematical model in the signal's phase space (Fig. 4 and system (19)) may lead to wrong conclusion.

Since loop filter inputs corresponding to both models are equal to $\frac{1}{4}$, initial VCO control inputs (and initial VCO frequencies) for both examples are the same.

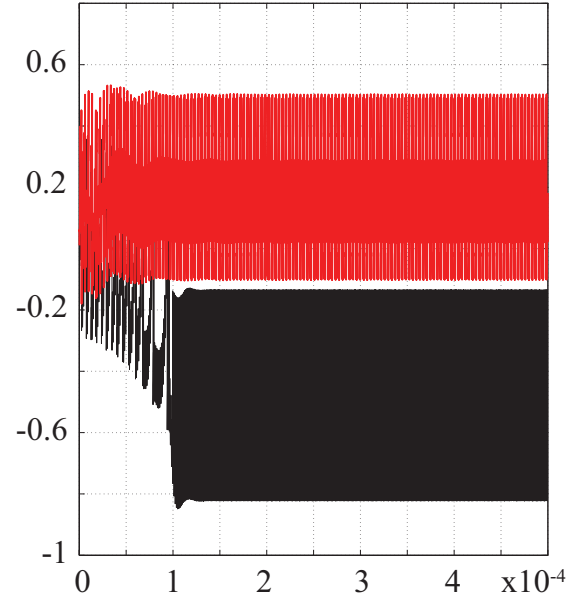


Fig. 9. Loop filter output: $m_1(t) = 1$; VCO free-running frequency $2.8283 \cdot 10^6$ rad/s; initial conditions of low-pass filters are 30 for red curve and zero for black curve; initial condition for loop filter is zero; $\omega_{lpf} = 1.2566 \cdot 10^6$; VCO phase shift is zero

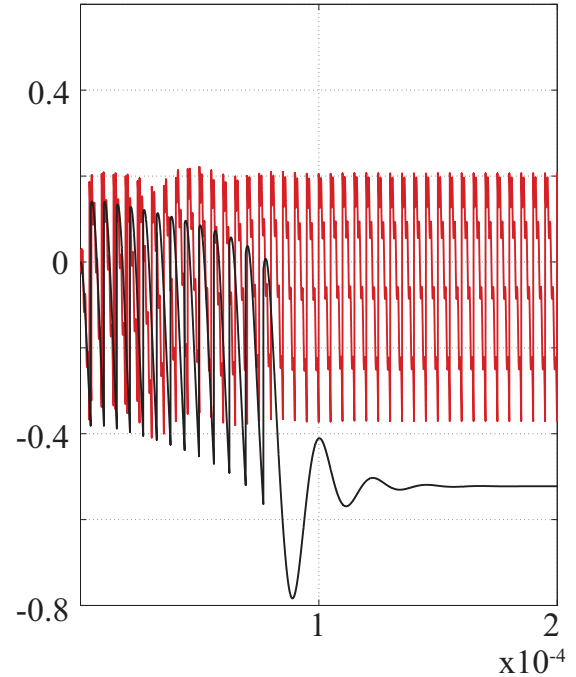


Fig. 10. Loop filter output: $m_1(t) \equiv 1$; Initial conditions of loop filter are zero; VCO phase shift is zero; VCO free-running frequency is $2.8433 \cdot 10^6$ rad/s; $\omega_{lpf} = 6.2832 \cdot 10^5$; red curve - taking into account signals with twice carrier frequency, black curve - taking into account only low frequency signals.

Therefore instead of one-dimensional stability ranges defined by $|\omega_{\Delta}|$ it is necessary to consider multi-dimensional stability domains taking into account initial phase difference $\{\theta_{\Delta}(0)\}$.

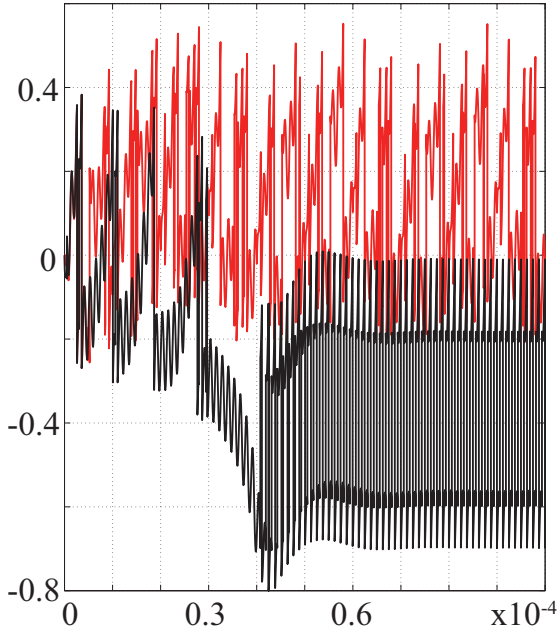


Fig. 11. Loop filter output: VCO free-running frequency are $2.7495 \cdot 10^6$ rad/s; VCO phase shift is zero; initial conditions of all filters are zero; $\omega_{lpf} = 1.2566 \cdot 10^6$; $m_1(t) = \text{sign}(\sin(2.7495 \cdot 10^6 t))$ – red curve, $m_1(t) = 1$ – black curve

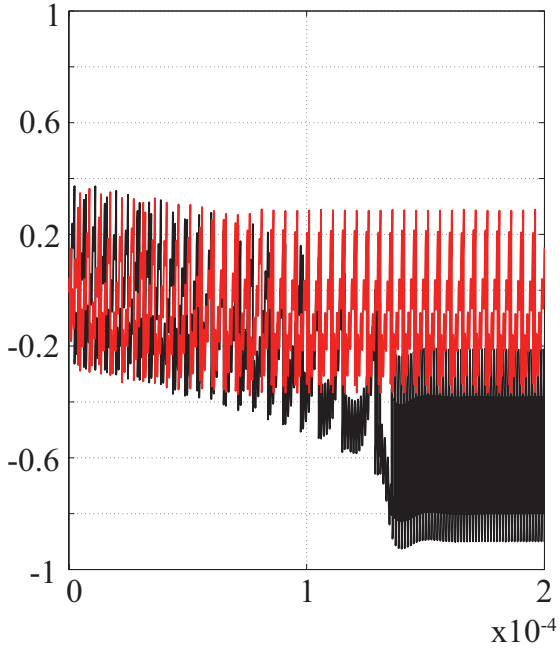


Fig. 12. Loop filter output for physical model: $m_1(t) = 1$; VCO free-running frequency is $2.8767 \cdot 10^6$ rad/s; VCO phase shift is for red curve and zero for black curve; $\omega_{lpf} = 1.2566 \cdot 10^6$; initial conditions of all filters are zero.

Here VCO free-running frequency is $\omega_{vco}^{free} = 2.5933 \cdot 10^6$, no data are being transmitted $m(t) = 1$, and initial loop filter state is zero $x(0) = \alpha_0(t) = 0$

Example 6. In Fig. 14. is shown that lowering corner frequency of the low-pass filter (therefore changing phase shift) may affect stability of the loop: while signals phase

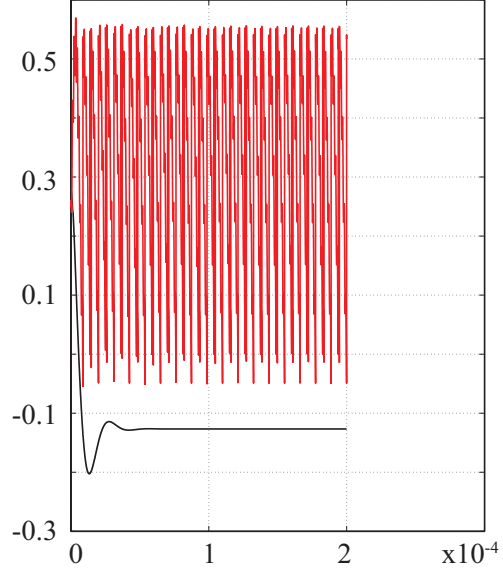


Fig. 13. Loop filter output $g(t)$ for signal's phase space model (black curve), physical model (red curve).

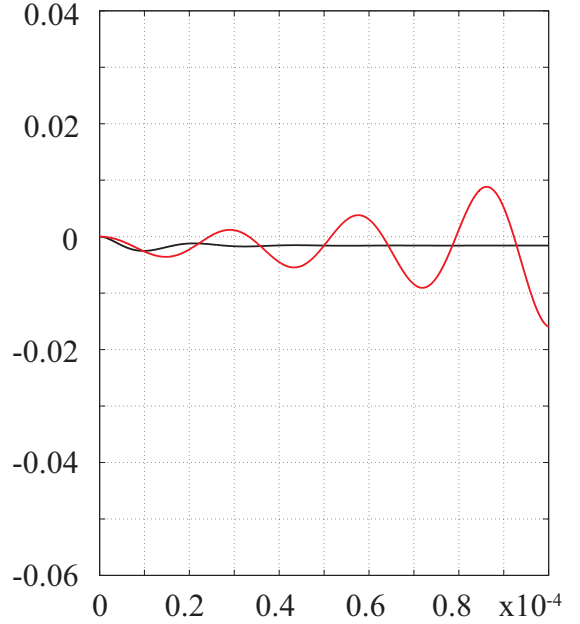


Fig. 14. Loop filter signal's phase model: $m_1(t) = 1$; VCO free-running frequency is $\omega_{ref} + 1000$; VCO phase shift is for red curve and zero for black curve; initial conditions of all filters are zero.

model (black) with $\omega_{lpf} = 6.2832 \cdot 10^5$ acquires lock, signals phase model (red) with $\omega_{lpf} = 1.5708 \cdot 10^5$ does not acquire lock.

4. CONCLUSION

In this survey various mathematical models of QPSK Costas loop are derived. It is shown that the consideration of simplified mathematical models, and the application of non rigorous methods of analysis (e.g., a simulation) can lead to wrong conclusions concerning the operability of *physical model* of Costas loop.

ACKNOWLEDGEMENTS

This work was supported by Russian Science Foundation (project 14-21-00041).

REFERENCES

- Abramovitch, D. (1990). Lyapunov redesign of analog phase-lock loops. *Communications, IEEE Transactions on*, 38(12), 2197–2202.
- Banerjee, T. and Sarkar, B. (2006). A new dynamic gain control technique for speed enhancement of digital phase locked loops (DPLLs). *Signal Processing*, 86, 1426–1434.
- Best, R., Kuznetsov, N., Kuznetsova, O., Leonov, G., Yuldashev, M., and Yuldashev, R. (2015). A short survey on nonlinear models of the classic Costas loop: rigorous derivation and limitations of the classic analysis. In *Proceedings of the American Control Conference*, 1296–1302. IEEE. doi:10.1109/ACC.2015.7170912. art. num. 7170912.
- Best, R., Kuznetsov, N., Leonov, G., Yuldashev, M., and Yuldashev, R. (2014). *Discontinuity and Complexity in Nonlinear Physical Systems*, volume 6, chapter Nonlinear analysis of phase-locked loop based circuits. Springer. doi:10.1007/978-3-319-01411-1_10.
- Best, R., Kuznetsov, N., Leonov, G., Yuldashev, M., and Yuldashev, R. (2016). Tutorial on dynamic analysis of the Costas loop. *Annual Reviews in Control*, 42, 27–49. doi:10.1016/j.arcontrol.2016.08.003.
- Bragin, V., Vagaitsev, V., Kuznetsov, N., and Leonov, G. (2011). Algorithms for finding hidden oscillations in nonlinear systems. The Aizerman and Kalman conjectures and Chua’s circuits. *Journal of Computer and Systems Sciences International*, 50(4), 511–543. doi:10.1134/S106423071104006X.
- Bueno, A., Ferreira, A., and Piqueira, J. (2010). Modeling and filtering double-frequency jitter in one-way master-slave chain networks. *IEEE transactions on circuits and systems-I*, 57(12), 3104–3111.
- Chang, F.J., Twu, S.H., and Chang, S. (1993). Global bifurcation and chaos from automatic gain control loops. *Circuits and Systems I: Fundamental Theory and Applications, IEEE Transactions on*, 40(6), 403–412.
- Chicone, C. and Heitzman, M. (2013). Phase-locked loops, demodulation, and averaging approximation time-scale extensions. *SIAM J. Applied Dynamical Systems*, 12(2), 674–721.
- Gardner, F. (1966). *Phaselock techniques*. John Wiley & Sons, New York.
- Goyal, P., Lai, X., and Roychowdhury, J. (2006). A fast methodology for first-time-correct design of PLLs using nonlinear phase-domain VCO macromodels. In *Proceedings of the 2006 Asia and South Pacific Design Automation Conference*, 291–296. doi:10.1109/ASPDAC.2006.1594697.
- Hedin, G., Holmes, J., Lindsey, W., and Woo, K. (1978). Theory of false lock in Costas loops. *Communications, IEEE Transactions on*, 26(1), 1–12.
- Hinz, M., Konenkamp, I., and Horneber, E.H. (2000). Behavioral modeling and simulation of phase-locked loops for RF front ends. In *Proc. 43rd BEE Midwest Symp. on Circuits and Systems*, 194–197. IEEE.
- Krylov, N. and Bogolyubov, N. (1947). *Introduction to non-linear mechanics*. Princeton Univ. Press, Princeton.
- Kudrewicz, J. and Wasowicz, S. (2007). *Equations of phase-locked loop. Dynamics on circle, torus and cylinder*. World Scientific.
- Kuznetsov, N., Kuznetsova, O., Leonov, G., Neittaanmaki, P., Yuldashev, M., and Yuldashev, R. (2014). Simulation of nonlinear models of QPSK Costas loop in Matlab Simulink. In *2014 6th International Congress on Ultra Modern Telecommunications and Control Systems and Workshops (ICUMT)*, volume 2015-January, 66–71. IEEE. doi:10.1109/ICUMT.2014.7002080.
- Kuznetsov, N. and Leonov, G. (2005). On stability by the first approximation for discrete systems. In *2005 International Conference on Physics and Control, PhysCon 2005*, volume Proceedings Volume 2005, 596–599. IEEE. doi:10.1109/PHYCON.2005.1514053.
- Kuznetsov, N., Leonov, G., and Seledzhi, S. (2011). Hidden oscillations in nonlinear control systems. *IFAC Proceedings Volumes*, 44(1), 2506–2510. doi:10.3182/20110828-6-IT-1002.03316.
- Leonov, G. and Kuznetsov, N. (2007). Time-varying linearization and the Perron effects. *International Journal of Bifurcation and Chaos*, 17(4), 1079–1107. doi:10.1142/S0218127407017732.
- Leonov, G. and Kuznetsov, N. (2013). Hidden attractors in dynamical systems. From hidden oscillations in Hilbert-Kolmogorov, Aizerman, and Kalman problems to hidden chaotic attractors in Chua circuits. *International Journal of Bifurcation and Chaos*, 23(1). doi:10.1142/S0218127413300024. art. no. 1330002.
- Leonov, G. and Kuznetsov, N. (2014). *Nonlinear Mathematical Models of Phase-Locked Loops. Stability and Oscillations*. Cambridge Scientific Publisher.
- Leonov, G., Kuznetsov, N., Yuldashev, M., and Yuldashev, R. (2012). Analytical method for computation of phase-detector characteristic. *IEEE Transactions on Circuits and Systems - II: Express Briefs*, 59(10), 633–647. doi:10.1109/TCSII.2012.2213362.
- Leonov, G., Kuznetsov, N., Yuldashev, M., and Yuldashev, R. (2015). Hold-in, pull-in, and lock-in ranges of PLL circuits: rigorous mathematical definitions and limitations of classical theory. *IEEE Transactions on Circuits and Systems-I: Regular Papers*, 62(10), 2454–2464. doi:10.1109/TCSI.2015.2476295.
- Leonov, G., Kuznetsov, N., Yuldashev, M., and Yuldashev, R. (2016). Computation of the phase detector characteristic of a QPSK Costas loop. *Doklady Mathematics*, 93(3), 348–353. doi:10.1134/S1064562416030236.
- Lindsey, W. (1972). *Synchronization systems in communication and control*. Prentice-Hall, New Jersey.
- Margaris, N. (2004). *Theory of the Non-Linear Analog Phase Locked Loop*. Springer Verlag, New Jersey.
- Mitropolsky, Y. and Bogolubov, N. (1961). *Asymptotic Methods in the Theory of Non-Linear Oscillations*. Gordon and Breach, New York.
- Olson, M. (1975). False-lock detection in Costas demodulators. *Aerospace and Electronic Systems, IEEE Transactions on*, AES-11(2), 180–182.
- Piqueira, J. and Monteiro, L. (2003). Considering second-harmonic terms in the operation of the phase detector for second-order phase-locked loop. *IEEE Transactions On Circuits And Systems-I*, 50(6), 805–809.

- Samoilenko, A. and Petryshyn, R. (2004). *Multifrequency Oscillations of Nonlinear Systems*. Mathematics and Its Applications. Springer.
- Sanders, J.A., Verhulst, F., and Murdock, J. (2007). *Averaging Methods in Nonlinear Dynamical Systems*. Springer.
- Sarkar, B.C., Sarkar, S.S.D., and Banerjee, T. (2014). Nonlinear dynamics of a class of symmetric lock range DPLLs with an additional derivative control. *Signal Processing*, 94, 631 – 641.
- Shakhgil'dyan, V. and Lyakhovkin, A. (1972). *Sistemy fazovoi avtopodstroiki chastoty (in Russian)*. Svyaz', Moscow.
- Shirahama, H., Fukushima, K., Yoshida, N., and Taniguchi, K. (1998). Intermittent chaos in a mutually coupled PLL's system. *Circuits and Systems I: Fundamental Theory and Applications, IEEE Transactions on*, 45(10), 1114–1117.
- Simon, M. (1978). The false lock performance of Costas loops with hard-limited in-phase channel. *Communications, IEEE Transactions on*, 26(1), 23–34.
- Stensby, J. (2002). Stability of false lock states in a class of phase-lock loops. In *System Theory, 2002. Proceedings of the Thirty-Fourth Southeastern Symposium on*, 133–137.
- Stensby, J. (1997). *Phase-Locked Loops: Theory and Applications*. Phase-locked Loops: Theory and Applications. Taylor & Francis.
- Stensby, J. (1989). False lock and bifurcation in Costas loops. *SIAM Journal on Applied Mathematics*, 49(2), pp. 420–431.
- Stensby, J. (2011). An exact formula for the half-plane pull-in range of a PLL. *Journal of the Franklin Institute*, 348(4), 671–684.
- Suarez, A. and Quere, R. (2003). *Stability Analysis of Nonlinear Microwave Circuits*. Artech House.
- Suarez, A., Fernandez, E., Ramirez, F., and Sancho, S. (2012). Stability and bifurcation analysis of self-oscillating quasi-periodic regimes. *IEEE Transactions on microwave theory and techniques*, 60(3), 528–541.
- Vendelin, G., Pavio, A., and Rohde, U. (2005). *Microwave Circuit Design Using Linear and Nonlinear Techniques*. Wiley.
- Viterbi, A. (1966). *Principles of coherent communications*. McGraw-Hill, New York.
- Wang, T.C., Chiou, T.Y., and Lall, S. (2008). Nonlinear phase-locked loop design using semidefinite programming. In *16th Mediterranean Conference on Control and Automation*, 1640–1645. IEEE.
- Watada, K., Endo, T., and Seishi, H. (1998). Shilnikov orbits in an autonomous third-order chaotic phase-locked loop. *IEEE transactions on circuits and systems-I*, 45(9), 979–983.
- Wiegand, C., Hedayat, C., and Hilleringmann, U. (2010). Non-linear behaviour of charge-pump phase-locked loops. *Advances in Radio Science*, 8, 161–166.
- Wu, N.E. (2002). Analog phaselock loop design using popov criterion. In *Proceedings of the 2002 American Control Conference (IEEE Cat. No. CH37301)*, volume 1, 16–18 vol.1. doi:10.1109/ACC.2002.1024771.
- Yoshimura, T., Iwade, S., Makino, H., and Matsuda, Y. (2013). Analysis of pull-in range limit by charge pump mismatch in a linear phase-locked loop. *Circuits and Systems I: Regular Papers, IEEE Transactions on*, 60(4), 896–907.